

# AIX-MARSEILLE UNIVERSITY

DOCTORAL SCHOOL: Physics and Material Science

PARTENAIRES DE RECHERCHE

Laboratoire MADIREL

Submitted with the view of obtaining the degree of doctor

Discipline: Material Science

Specialty: Characterisation of porous materials

Paul A. Iacomì

Titre de la thèse: sous-titre de la thèse

Defended on JJ/MM/AAAA in front of the following jury:

Prénom NOM	Affiliation	Rapporteur
Prénom NOM	Affiliation	Rapporteur
Prénom NOM	Affiliation	Examineur
Prénom NOM	Affiliation	Examineur
Prénom NOM	Affiliation	Examineur
Prénom NOM	Affiliation	Directeur de thèse

National thesis number: 2017AIXM0001/001ED62



This work falls under the conditions of the [Creative Commons Attribution License - No commercial use - No modification 4.0 International](https://creativecommons.org/licenses/by-nc-nd/4.0/).

# Abstract

Abstract is here.

# Acknowledgements

Acknowledgements go here

# Contents

<b>Abstract</b>	<b>iii</b>
<b>Acknowledgements</b>	<b>iv</b>
<b>1 Building a framework for adsorption data processing</b>	<b>1</b>
1.1 Introduction . . . . .	1
1.2 pyGAPS overview . . . . .	1
1.2.1 Intended use cases . . . . .	1
1.2.2 Core structure . . . . .	2
1.2.3 Creation of an Isotherm . . . . .	3
1.2.4 Workflow . . . . .	3
1.2.5 Units . . . . .	5
1.3 Isotherm characterisation and fitting . . . . .	5
1.3.1 Mathematical descriptions of isotherms . . . . .	5
1.3.2 Specific surface area and pore volume calculations . . . . .	11
1.3.3 Assessing porosity . . . . .	19
1.4 Case studies . . . . .	25
1.4.1 Routine characterization of a MOF sample . . . . .	25
1.4.2 Analysis of a carbon sample for gas separation applications . . . . .	27
1.5 Conclusion . . . . .	30
<b>2 Extending bulk analysis of porous compounds through calorimetry</b>	<b>31</b>
2.1 Introduction . . . . .	31
2.2 Literature . . . . .	31
2.3 Method . . . . .	32
2.4 Results and discussion . . . . .	32
2.5 Conclusion . . . . .	32
<b>3 Exploring the impact of synthesis and defects on adsorption measurements</b>	<b>34</b>
3.1 Introduction . . . . .	34
3.2 Literature . . . . .	34
3.3 Method . . . . .	34
3.4 Results and discussion . . . . .	34
3.5 Conclusion . . . . .	34
<b>4 Exploring the impact of material form on adsorption measurements</b>	<b>36</b>
4.1 Introduction . . . . .	36
4.2 Shaping in context . . . . .	36
4.3 Synthesis, shaping and characterisation . . . . .	38
4.3.1 Material Synthesis . . . . .	38

## Contents

4.3.2	Shaping Procedure . . . . .	39
4.3.3	Characterisation of powders and pellets . . . . .	39
4.3.4	Sample activation for adsorption . . . . .	39
4.4	Results and discussion . . . . .	39
4.4.1	Thermal stability . . . . .	39
4.4.2	Adsorption isotherms at 77K and room temperature . . . . .	41
4.4.3	Room temperature gas adsorption and microcalorimetry . . . . .	41
4.4.4	Vapour adsorption . . . . .	49
4.5	Conclusion . . . . .	51
<b>5</b>	<b>Exploring novel behaviours</b>	<b>57</b>
5.1	Introduction . . . . .	57
5.2	Literature . . . . .	57
5.3	Method . . . . .	57
5.4	Results and discussion . . . . .	57
5.5	Conclusion . . . . .	57
	<b>Common characterisation techniques</b>	<b>59</b>
1	Thermogravimetry . . . . .	59
2	Bulk density determination . . . . .	59
3	Skeletal density determination . . . . .	59
4	Nitrogen physisorption at 77 K . . . . .	60
5	Vapour physisorption at 298 K . . . . .	60
6	Gravimetric isotherms . . . . .	60
	<b>Synthesis method of referenced materials</b>	<b>62</b>
1	Takeda 5A reference carbon . . . . .	62
2	MCM-41 controlled pore glass . . . . .	62
3	Zr fumarate MOF . . . . .	62
4	UiO-66(Zr) for defect study . . . . .	62
5	UiO-66(Zr) for shaping study . . . . .	63
6	MIL-100(Fe) for shaping study . . . . .	63
7	MIL-127(Fe) for shaping study . . . . .	63
	<b>Complete adsorption dataset for shaping study</b>	<b>64</b>
1	Calorimetry dataset UiO-66(Zr) . . . . .	64
2	Calorimetry MIL-100(Fe) . . . . .	65
3	Calorimetry MIL-127(Fe) . . . . .	68

# 1 Building a framework for adsorption data processing

## 1.1 Introduction

Historically, the processing of isotherms was done by hand, with large worksheets being used for the calculations. As an example, we point out that one of the initial limitations of the BJH method was that each point had to be determined with an approximation of critical pore radius, due to the tedious work involved in the calculation.<sup>(1)</sup>

The advent of computers meant that the calculations could be performed quickly and reliably and led to the introduction of more complex methods for isotherm processing, such as the DFT method for pore size distribution.<sup>(2,3)</sup> Commercial adsorption equipment which offers the users a complete software solution for any isotherm calculations is now commonplace and makes obtaining reports of desired properties for measured materials a matter of minutes.

Given the current ubiquitousness of adsorption as a characterisation method, particularly for investigating surfaces and porous compounds, there is a large pool of data published in the scientific community. Key performance indicators such as specific surface area, working capacity and pore volume are commonly reported in scientific literature and used as benchmarking tools for comparing performance.

Recent efforts have also focused on building a database of adsorption isotherms,<sup>(4)</sup> to offer a searchable pool of standardised behaviours on different materials. This serves as both a useful reference for comparing synthesised compounds, as well as a method for quickly finding suitable materials which have the desired properties for a particular application.

In this chapter an open-source software package is presented, which is released under an MIT licence and written in Python, intended to be used for manipulation, storage, visualisation and processing of adsorption isotherms. Developed internally at the MADIREL Laboratory in Marseilles, the software is aimed to give users a powerful yet easy to use package that can perform the kind of processing usually offered by commercial software.

## 1.2 pyGAPS overview

### 1.2.1 Intended use cases

The software was imagined for use in two types of scenario. First, as a command line interface, in environments such as IPython and Jupyter. The typical user working in these environments is likely to be processing a small batch of results at one time, and is interested in obtaining the results in graphical form. For this type of application,

the framework should provide an unobtrusive way of importing the user data, as well as present an API which does not require extensive knowledge of processing methods. Finally, a powerful graphing environment is required which will allow the user to visualise their original dataset and results.

The second envisaged application is related to bulk data processing. Requirements here shift towards parameter control, scripting and extensibility. The framework API should offer the option to change implicit parameters, select calculation limits and return the results in a numerical form for further processing. This type of application is also likely to require storage of isotherms in a database or under other types of data files.

## 1.2.2 Core structure

In order to offer a clear structuring of functionality, **pyGAPS** introduces several classes which abstract data and functionality for facile interaction. The classes are intuitively named: **Isotherm**, **Sample** and **Adsorbent**.

### The Isotherm class

The **Isotherm** class is a representation of an adsorption isotherm i.e. a function of the amount adsorbed, or loading, with pressure at a fixed temperature. The class also contains other information relating to the isotherm, such as the material name and batch it describes, the adsorbate used and other user-defined properties.

Because the aforementioned relationship can be either a physical measurement defined by individual pressure-loading pairs or a model, describing the relationship as a function rather than discrete data, the **Isotherm** class is used as a parent class for two subclasses: **PointIsotherm**, describing datapoints and **ModelIsotherm** containing a model such as Henry, Langmuir etc., which encapsulate the respective functionality. The two classes are interchangeable as they share most methods and properties. Once an instance of an **Isotherm** class is created, it can then be used for the processing, conversion and graphing capabilities of **pyGAPS**.

### The Sample class

The isotherm classes contain the name and batch of the sample they are measured on in a string format. The user might want to specify other information about the material, such as the date of synthesis or the material's density, as well as store this information in the database. For this case, **pyGAPS** provides the **Sample** class. The framework uses the string values in the isotherm to connect an **Isotherm** instance to a specific **Sample**.

### The Adsorbate class

Finally, in order for many of the calculations included in **pyGAPS** to be performed, properties of the adsorbate used are needed e.g. liquid density, vapour pressure etc. The **Adsorbate** class is provided for this purpose, which is connected to an **Isotherm** class similarly to a **Sample**. The physical properties are either calculated in the background



through an equation of state, either the open source CoolProp library<sup>(5)</sup> or the NIST-made REFPROP.<sup>(6)</sup> The properties can also be retrieved from the internal database or specified by the user.

### 1.2.3 Creation of an Isotherm

An **Isotherm** can be created either from the command line directly or through an import from a supported format. For the direct creation, the code takes two kinds of inputs: the data itself, in the form of a `pandas.DataFrame`, and the isotherm parameters describing it. Only four parameters are strictly required: the material name, the material batch, the adsorbate used and the experimental temperature. Other parameters can be passed as well and will be stored in the isotherm class.

Listing 1.1: Creating the `DataFrame`

```
1 isotherm_data = pandas.DataFrame({
2     'pressure' : [1, 2, 3, 4, 5, 3, 2],
3     'loading'  : [1, 2, 3, 4, 5, 3, 2],
4     'enthalpy' : [15, 15, 15, 15, 15, 15, 15],
5     'xrd_peak_1' : [0, 0, 1, 2, 2, 1, 0],
6 })
```

The `DataFrame` must contain a column containing the pressure points and one containing the corresponding loading points of the isotherm. Other columns can also be passed, when secondary data such as enthalpy of adsorption is present at each measurement point. These columns will be saved in the case of the `PointIsotherm` class and can be plotted afterwards.

If no unit data is specified in the constructor, the framework will assume that the isotherm is in units of  $\text{mmol g}^{-1}$  loading as a function of bar. Both the units and the basis can be specified, as it is explained in a latter section.

Finally, the data is saved in the newly created class or used to generate parameters for a model such as BET, Langmuir, etc., in the case of a `PointIsotherm` and `ModelIsotherm` respectively. It should be noted that the creation of `Sample` and `Adsorbate` instances is similar.

Alternatively, the isotherm can be imported from a file containing a format that is recognised by `pyGAPS`. Parsing from suitably structured JSON, CSV and Excel files is supported.

### 1.2.4 Workflow

Once an isotherm object is created, it will be used for all further processing. The class contains methods which can be used to inspect the data visually, or retrieve parts of the isotherm such as the adsorption or desorption branches with user-chosen limits or units. Singular values of pressure or loading can be calculated, either through interpolation in the case of a `PointIsotherm` or by evaluation of the internal model in the `ModelIsotherm`. For an isotherm with datapoints, these can also be converted into different units or modes.

Listing 1.2: Creating the PointIsotherm

```

1 point_isotherm = pygaps.PointIsotherm(
2
3     # First the pandas.DataFrame with the points
4     # and the keys to what the columns represent.
5
6     isotherm_data,
7
8     loading_key='loading',          # The loading column
9     pressure_key='pressure',        # The pressure column
10    other_keys=['enthalpy',
11               'xrd_peak_1'],       # The columns containing other data
12
13    # Some of the unit parameters can be
14    # specified if desired.
15
16    pressure_mode='absolute',        # absolute pressure
17    pressure_unit='bar',              # with units of bar
18    adsorbent_basis='mass',          # adsorbent mass basis
19    adsorbent_unit='kg',              # with units of kg
20    loading_basis='mass',            # loading mass basis
21    loading_unit='g',                # with units of g
22
23    # Finally the isotherm description
24    # parameters are passed.
25
26    'sample_name' : 'carbon',        # Required
27    'sample_batch' : 'X1',           # Required
28    'adsorbate' : 'nitrogen',        # Required
29    't_exp' : 77,                    # Required
30    't_act' : 150,                   # Recognised / named
31    'user' : 'Username',             # Recognised / named
32    'DOI' : '10.000/mydoi',          # Unknown / user specific
33 )

```

Characterisation functions take a single isotherm object as their first parameter. This is the case for the BET area, Langmuir area, t-plot,  $\alpha_s$  plot, and pore size distribution methods. These characterisation functions attempt to automate as much of the process as possible. For example, the BET area limits are automatically calculated using the Rouquerol<sup>(7)</sup> method, with all the checks implemented into the code. In another example the straight line sections of the t-plot are determined automatically through a calculation of the second derivative of the transformed isotherm. For detailed control, there is an option to specify options for each individual method, such as manual BET limits, different thickness functions for the t-plot or Kelvin-based mesoporous pore distribution methods, custom parameters for the Horvath-Kawazoe microporous pore distribution, custom DFT or NLDFIT kernels and more. The results are returned in a dictionary or can be directly graphed if the `verbose` parameter is passed.

### 1.2.5 Units

When computers work with physical data, units are often a matter that introduces confusion. Here we explain how **pyGAPS** handles units and other physical world concepts such as relative pressure and mass or volume basis.

The following dimensions can be specified for an Isotherm: the measurement *pressure*, the quantity of guest adsorbed or *loading* and the amount of adsorbent material the loading is reported on, or *adsorbent*.

Pressure can be reported either in an absolute value, in several common units such as bar, torr, Pa, or as *relative pressure*, the pressure divided by the saturation vapour pressure of the adsorbate at the respective measurement temperature. Conversions between the two modes are automatic and handled internally.

Both the *loading* and *adsorbent* can be reported in three different bases: a molar basis, a mass basis or a volume basis. Within each basis different units are recognised and can be easily converted. The conversions between bases can also easily performed if the required conversion factors (i.e. molar mass and density) are available. For *loading*, these factors are automatically calculated internally, while for the *adsorbent* they should be provided by the user in the respective **Sample** class.

## 1.3 Isotherm characterisation and fitting

### 1.3.1 Mathematical descriptions of isotherms

A lot of effort was put into attempting to describe the phenomenon of adsorption using a simple model. Through a mathematical understanding, the underlying mechanisms of adsorption can be understood. Unfortunately, the plethora of isotherm features and shapes can only be truly recreated by molecular simulation, which requires an exact knowledge of the adsorbent structure and its interaction with the adsorbed gas. Nevertheless, great strides have been taken to obtain several models which can be useful when fitted to measured isotherms for obtaining simple parameters which are representative of physical factors such as guest-host interaction, surface area, pore size, total pore volume and others. More importantly, it allows us to numerically compare measured isotherms.

A page of figures for different models can be seen in Figure 1.1.

change  
location

#### The Henry model

The simplest method of describing adsorption on a surface is Henry's law. It assumes only interactions with the adsorbate surface and is described by a linear dependence of adsorbed amount with increasing pressure.

$$n_a(p) = K_H p \quad (1.1)$$

Physically, Henry's law is unrealistic as adsorption sites will saturate at higher pressures. However, the constant  $K_H$ , or Henry's constant, can be thought of as a measure

of the strength of the interaction of the probe gas with the surface. At very low concentrations of gas there is a theoretical requirement for the applicability of Henry's law. Therefore, most models reduce to equation 1.1 as  $\lim_{p \rightarrow 0} n(p)$ .

### Langmuir and multi-site Langmuir model

The Langmuir theory, <sup>(8)</sup> proposed at the start of the 20th century, states that adsorption takes place on specific sites on a surface, until all sites are occupied. It is derived based on several assumptions:

- All sites are equivalent and have the same chance of being occupied.
- Each adsorbate molecule can occupy one adsorption site.
- There are no interactions between adsorbed molecules.
- The rates of adsorption and desorption are proportional to the number of sites currently free and currently occupied, respectively.
- Adsorption is complete when all sites are filled.

Using these assumptions we can define rates for both adsorption and desorption. The adsorption rate (equation 1.2) will be proportional to the number of sites available on the surface, as well as the number of molecules in the gas, which is given by pressure. The desorption rate, on the other hand, will be proportional to the number of occupied sites and the energy of adsorption (equation 1.3). It is also useful to define  $\theta = n_a/n_a^m$  as the surface coverage, the number of sites occupied divided by the total sites. At equilibrium, the rate of adsorption and the rate of desorption are equal, therefore the two equations can be combined. The equation can then be arranged to obtain an expression for the loading called the Langmuir equation (1.5).

$$v_a = k_a p (1 - \theta) \tag{1.2}$$

$$v_d = k_d \theta \exp\left(-\frac{E}{RT}\right) \tag{1.3}$$

$$k_a p (1 - \theta) = k_d \theta \exp\left(-\frac{E}{RT}\right) \tag{1.4}$$

$$n_a(p) = n_a^m \frac{Kp}{1 + Kp} \tag{1.5}$$

The Langmuir constant  $K$  is the product of the individual desorption and adsorption constants  $k_a$  and  $k_d$  and exponentially related to the energy of adsorption  $\exp(-E/RT)$ .

A common extension to the Langmuir model is to consider the experimental isotherm to be the sum of several Langmuir-type isotherms, each with specific maximum coverage and affinities. The underlying assumption is that the adsorbent has several distinct types of homogeneous adsorption sites and a Langmuir equation is used for each. This

is particularly applicable in cases where the structure of the adsorbent suggests that different types of sites are present, such as in crystalline materials of variable chemistry like zeolites and MOFs. The resulting isotherm equation is:

$$n_a(p) = \sum_i n_{a,i}^m \frac{K_i p}{1 + K_i p} \quad (1.6)$$

In practice, only up to three adsorption sites are usually considered.

### BET model

The BET model<sup>(9)</sup> assumes that adsorption takes place on the surface of the material in incremental layers according to several assumptions:

- The adsorption sites are equivalent, and therefore the surface is heterogeneous.
- There are no lateral interactions between adsorbed molecules.
- The adsorption takes place in layers, with adsorbed molecules acting as sites for the next layer.
- The adsorption energy of a molecule on the second and higher layers is the same and equals the condensation energy of the adsorbent  $E_L$ .

A particular surface percentage  $\theta_x$  is occupied with x layers. For each layer at equilibrium, the adsorption and desorption rates must be equal. We can then apply the Langmuir theory for each layer.

$$k_{a1}p\theta_0 = k_{d1}\theta_1 \exp\left(-\frac{E_1}{RT}\right) \quad (1.7)$$

$$k_{a2}p\theta_1 = k_{d2}\theta_2 \exp\left(-\frac{E_L}{RT}\right) \quad (1.8)$$

$\vdots$

$$k_{ai}p\theta_{i-1} = k_{di}\theta_i \exp\left(-\frac{E_L}{RT}\right) \quad (1.9)$$

Since we are assuming that all layers beside the first have the same properties, we can define  $g = k_{d2}k_{a2} = k_{d3}k_{a3} = \dots$ . The coverage for each layer  $\theta$  can now be expressed in terms of  $\theta_0$ .

better  
struc-  
ture

$$\theta_1 = y\theta_0 \quad \text{where} \quad y = p \frac{k_{a1}}{k_{d1}} \exp\left(-\frac{E_1}{RT}\right) \quad (1.10)$$

$$\theta_2 = x\theta_1 \quad \text{where} \quad x = \frac{p}{g} \exp\left(-\frac{E_L}{RT}\right) \quad (1.11)$$

$$\theta_3 = x\theta_2 = x^2\theta_1 \quad (1.12)$$

$$\vdots$$

$$\theta_i = x^{i-1}\theta_1 = yx^{i-1}\theta_0 \quad (1.13)$$

A constant C may be defined such that

$$C = \frac{y}{x} = \frac{k_{a1}}{k_{d1}} g \exp\left(\frac{E_1 - E_L}{RT}\right) \theta_i = Cx^i\theta_0 \quad (1.14)$$

For all the layers, the equations can be summed:

$$\frac{n}{n_m} = \sum_{i=1}^{\infty} i\theta^i = C \sum_{i=1}^{\infty} ix^i\theta_0 \quad (1.15)$$

And since

$$\theta_0 = 1 - \sum_1^{\infty} \theta_i \sum_{i=1}^{\infty} ix^i = \frac{x}{(1-x)^2} \quad (1.16)$$

Then we obtain the BET equation

$$n_a(p) = n_a^m \frac{K_ap}{(1 - K_bp)(1 - K_bp + K_ap)} \quad (1.17)$$

check  
equa-  
tion

The equation reduces to the Langmuir equation (1.5) when

### Toth model

The Toth model is an empirical modification to the Langmuir equation (1.5) which introduces a power parameter for the denominator leading to the following formula:

$$n_a(p) = n_a^m \frac{Kp}{[1 + (Kp)^t]^{1/t}} \quad (1.18)$$

The parameter  $t$  is a measure of the system heterogeneity. Thanks to this additional parameter, the Toth equation can accurately describe a large number of adsorbent/adsorbate systems and is recommended as the first choice of isotherm equation for fitting

isotherms of many adsorbents such as hydrocarbons, carbon oxides, hydrogen sulphide and alcohols on activated carbons but also zeolites. It is worth noting that the equation no longer reduces to the Henry law at low loading and therefore is theoretically inconsistent.

### Temkin model

The Temkin adsorption isotherm,<sup>(10)</sup> like the Langmuir model, considers a surface with  $n_a^m$  identical adsorption sites, but takes into account adsorbate-adsorbate interactions by assuming that the heat of adsorption is a linear function of the coverage. This expression for the Temkin isotherm is derived using a mean-field argument and uses an asymptotic approximation to obtain an explicit equation for the loading.<sup>(11)</sup>

$$n_a(p) = n_a^m \frac{Kp}{1 + Kp} + n_a^m \theta \left( \frac{Kp}{1 + Kp} \right)^2 \left( \frac{Kp}{1 + Kp} - 1 \right) \quad (1.19)$$

Here,  $n_a^m$  and  $K$  have the same physical meaning as in the Langmuir model. The additional parameter  $\theta$  describes the strength of the adsorbate-adsorbate interactions ( $\theta < 0$  for attractions).

### Jensen-Seaton model

When modelling adsorption in micropores, a requirement was highlighted by Jensen and Seaton in 1996<sup>(12)</sup> that at sufficiently high pressures the adsorption isotherm should not reach a horizontal plateau corresponding to saturation but that this asymptote should continue to rise due to the compression of the adsorbate in the pores. They developed a semi-empirical equation to describe this phenomenon based on a function that interpolates between two asymptotes: the Henry's law asymptote at low pressure and an asymptote reflecting the compressibility of the adsorbate at high pressure.

$$n(p) = K_H p \left( 1 + \frac{K_H p}{[a(1+bp)]^c} \right)^{(-1/c)} \quad (1.20)$$

Here  $K_H$  is the Henry constant,  $b$  is the compressibility of the adsorbed phase and  $c$  an empirical constant.

The equation can be used to model both absolute and excess adsorption as the pore volume can be incorporated into the definition of  $b$ , although this can lead to negative adsorption slopes for the compressibility asymptote. This equation has been found to provide a better fit for experimental data from microporous solids than the Langmuir or Toth equation, in particular for adsorbent/adsorbate systems with high Henry's constants where the amount adsorbed increases rapidly at relatively low pressures and then slows down dramatically.

### Quadratic model

The quadratic adsorption isotherm<sup>(13)</sup> exhibits an inflection point. The loading is convex at low pressures but changes concavity as it saturates, yielding an S-shape. The S-shape can be explained by adsorbate-adsorbate attractive forces; the initial convexity is due to a cooperative effect of adsorbate-adsorbate attractions aiding in the recruitment of additional adsorbate molecules.

$$n(p) = n_a^m \frac{(K_a + 2K_b p)p}{1 + K_a p + K_b^2 p^2} \quad (1.21)$$

The parameter  $K_a$  can be interpreted as the Langmuir constant; the strength of the adsorbate-adsorbate attractive forces is embedded in  $K_b$ .

### Virial model

A virial isotherm model attempts to fit the measured data to a factorized exponent relationship between loading and pressure.<sup>(14)</sup>

$$p = n \exp(K_1 n^0 + K_2 n^1 + K_3 n^2 + K_4 n^3 + \dots + K_i n^{i-1}) \quad (1.22)$$

It has been applied with success to describe the behaviour of standard as well as supercritical isotherms. The factors are usually empirical, although some relationship with physical properties can be determined: the first constant is related to the Henry constant at zero loading, while the second constant is a measure of the interaction strength with the surface.

$$K_1 = -\ln K_{H,0} \quad (1.23)$$

In practice, besides the first constant, only 2-3 factors are used.

### Vacancy solution theory models

As a part of the Vacancy Solution Theory (VST) family of models, it is based on concept of a “vacancy” species, denoted  $v$ , and assumes that the system consists of a mixture of these vacancies and the adsorbate.

The VST model is defined as follows:

- A vacancy is an imaginary entity defined as a vacuum space which acts as the solvent in both the gas and adsorbed phases.
- The properties of the adsorbed phase are defined as excess properties in relation to a dividing surface.



- The entire system including the adsorbent are in thermal equilibrium however only the gas and adsorbed phases are in thermodynamic equilibrium.
- The equilibrium of the system is maintained by the spreading pressure which arises from a potential field at the surface

It is possible to derive expressions for the vacancy chemical potential in both the adsorbed phase and the gas phase, which when equated give the following equation of state for the adsorbed phase:

$$\pi = -\frac{R_g T}{\sigma_v} \ln y_v x_v \quad (1.24)$$

where  $y_v$  is the activity coefficient and  $x_v$  is the mole fraction of the vacancy in the adsorbed phase. This can then be introduced into the Gibbs equation to give a general isotherm equation for the Vacancy Solution Theory where  $K_H$  is the Henry's constant and  $f(\theta)$  is a function that describes the non-ideality of the system based on activity coefficients:

$$p = \frac{n_{ads}}{K_H} \frac{\theta}{1 - \theta} f(\theta) \quad (1.25)$$

The general VST equation requires an expression for the activity coefficients. The Wilson<sup>(15)</sup> equation can be used, which expresses the activity coefficient in terms of the mole fractions of the two species (adsorbate and vacancy) and two constants  $\Lambda_{1v}$  and  $\Lambda_{1v}$ . The equation becomes:

$$p = \left( \frac{n_{ads}}{K_H} \frac{\theta}{1 - \theta} \right) \left( \Lambda_{1v} \frac{1 - (1 - \Lambda_{v1})\theta}{\Lambda_{1v} + (1 - \Lambda_{1v})\theta} \right) \exp \left( -\frac{\Lambda_{v1}(1 - \Lambda_{v1})\theta}{1 - (1 - \Lambda_{v1})\theta} - \frac{(1 - \Lambda_{1v})\theta}{\Lambda_{1v} + (1 - \Lambda_{1v})\theta} \right) \quad (1.26)$$

Cochran<sup>(16)</sup> developed a simpler, three parameter equation based on the Flory-Huggins equation for the activity coefficient. The equation for then becomes:

$$p = \left( \frac{n_{ads}}{K_H} \frac{\theta}{1 - \theta} \right) \exp \frac{\alpha_{1v}^2 \theta}{1 + \alpha_{1v} \theta} \quad \text{where} \quad \alpha_{1v} = \frac{\alpha_1}{\alpha_v} - 1 \quad (1.27)$$

Here  $\alpha_1$  and  $\alpha_v$  are the molar areas of the adsorbate and the vacancy respectively.

### 1.3.2 Specific surface area and pore volume calculations

#### BET surface area

The BET method<sup>(9)</sup> for determining surface area is the recommended IUPAC method<sup>(17)</sup> to calculate the surface area of a porous material. It is generally applied on isotherms

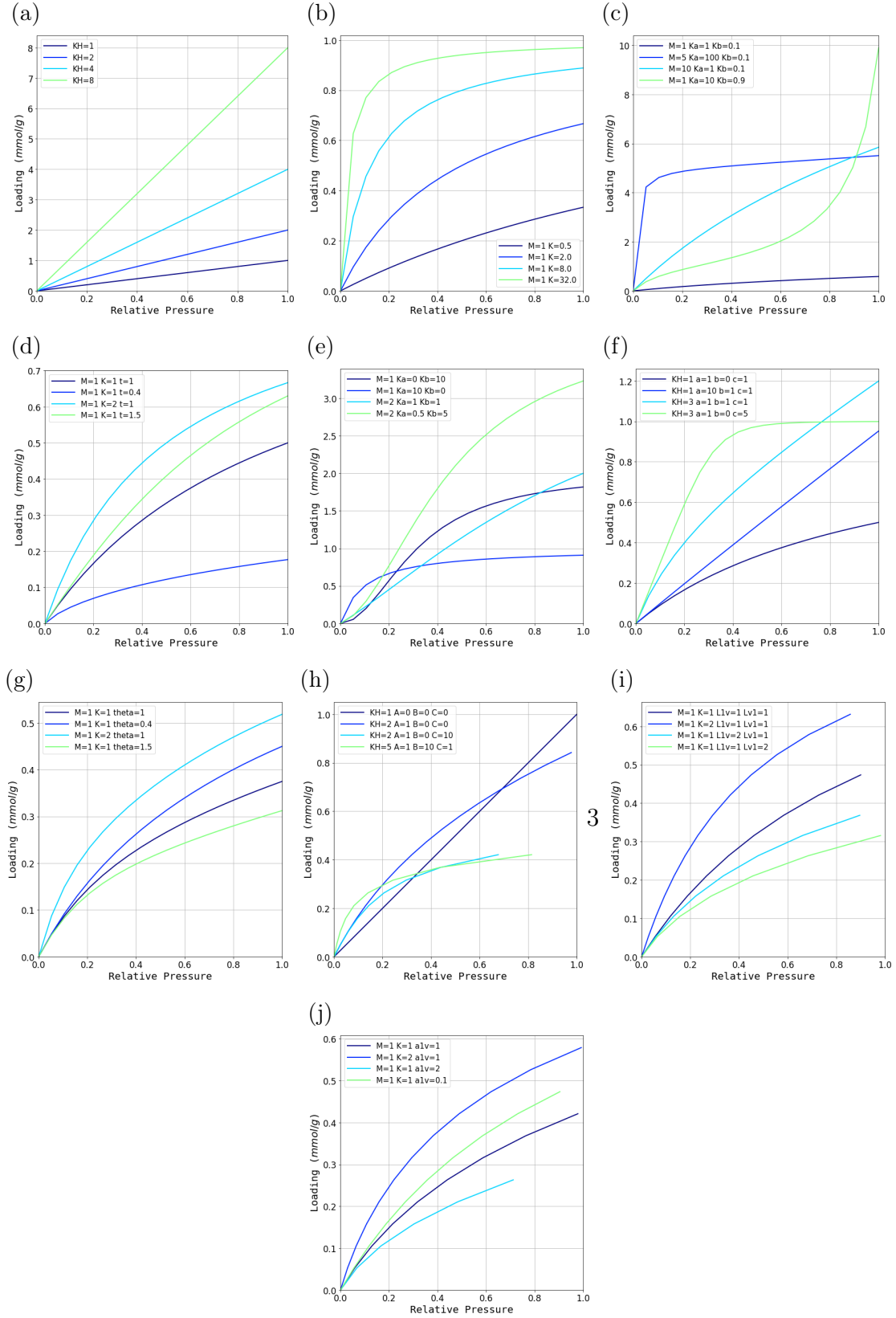


Figure 1.1: Examples of models

obtained through N<sub>2</sub> adsorption at 77 K, although other adsorbates (Ar at 77 K or 87 K, Kr at 77 K, CO<sub>2</sub> at 293 K) have been used. In principle, any probe with an adsorption behaviour which can be described through the BET equation in the low pressure regime can be used.

As mentioned before, the method assumes that the adsorption takes place on the surface of the material in incremental layers according to the BET equation (1.17). Even if the adsorbent is porous, the initial amount adsorbed (usually between 0.05 - 0.4  $p/p_0$ ) can be modelled through the equation written in its linear form:

$$\frac{p/p_0}{n_{ads}(1 - p/p_0)} = \frac{1}{n_m C} + \frac{C - 1}{n_m C} (p/p_0) \quad (1.28)$$

If we plot the isotherm points as  $(p/p_0)/n_{ads}(1 - p/p_0)$  versus  $p/p_0$ , a linear region can usually be found. The slope and intercept of this line can then be used to calculate  $n_m$ , the amount adsorbed at the statistical monolayer, as well as  $C$ , the BET constant.

$$n_m = \frac{1}{s + i} \quad C = \frac{s}{i} + 1 \quad (1.29)$$

The surface area can then be calculated by using the moles adsorbed at the statistical monolayer. If the specific area taken by one of the adsorbate molecules on the surface is known, it is inserted in the following equation together with Avogadro's number:

$$a_{BET} = n_m A_N \sigma \quad (1.30)$$

While a standard for surface area determinations, the BET area should be used with care, as the assumptions made in its calculation may not hold. To augment the validity of the BET method, Rouquerol<sup>(7)</sup> proposed several checks to ensure that the BET region selected is valid:

- The BET ( $C$ ) obtained should be positive;
- In the corresponding Rouquerol plot where  $n_{ads}(1 - p/p_0)$  is plotted with respect to  $p/p_0$ , the points chosen for BET analysis should be strictly increasing;
- The loading at the statistical monolayer should be situated within the limits of the BET region.

All these checks are implemented in **pyGAPS**. Regardless, the BET surface area should still be interpreted carefully. Since adsorption takes place on the pore surface, microporous materials which have pores of similar or smaller size as the probe molecule used will not give a realistic surface area. Furthermore, the cross-sectional area of the molecule on the surface cannot be guaranteed. For example, nitrogen has been known to adopt

a different conformation on the surface of some materials due to inter-molecular forces, which effectively lowers its cross-sectional area.<sup>(7)</sup>

In `pyGAPS`, starting from an isotherm object, it is easy to calculate the BET area by using the code in Listing 1.3. The framework automatically applies the Rouquerol rules to find the optimum pressure range and returns the results as a dictionary. The `verbose=True` option prints a short text with all the calculation variables as well as the BET and Rouquerol plots (Figure 1.2). The user can override automatic pressure range selection by using the range parameter (`limits=(0.05, 0.3)`).

Listing 1.3: Calculating a BET area

```
1 area_dict = pygaps.area_BET(isotherm, verbose=True)
```

```
BET surface area: a = 1277 m2/g
Minimum pressure point chosen is 0.005 and maximum is 0.034
The slope of the BET fit:      s = 76.344
The intercept of the BET fit:  i = 0.052
BET constant:                  C = 1463
Amount for a monolayer:       n = 0.01309 mol/g
```

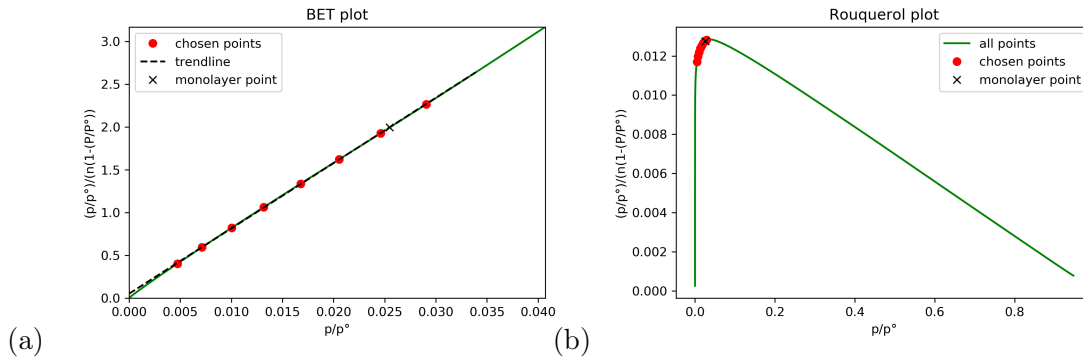


Figure 1.2: Output from the BET area function (a) the BET plot showing the selected points for fitting the equation, as well as the location of the statistical monolayer and (b) the Rouquerol plot for this calculation.

## Langmuir surface area

The Langmuir equation (1.5) can be also be expressed in a linear form by rearranging it as:

$$\frac{p}{n} = \frac{1}{Kn_m} + \frac{p}{n_m} \quad (1.31)$$

Assuming the data can be fitted with a Langmuir model, by plotting  $P/n$  against pressure, a line will be obtained. The slope and intercept of this line can then be used

to calculate  $n_m$ , the amount adsorbed at the monolayer, as well as  $K$ , the Langmuir constant.

$$n_m = \frac{1}{s} \qquad K = \frac{1}{i * n_m} \qquad (1.32)$$

The surface area can then be calculated by using the moles adsorbed at the monolayer using the same assumptions as when obtaining the BET surface area.

$$a_{Langmuir} = n_m A_N \sigma \qquad (1.33)$$

The Langmuir method for determining surface area assumes that only a single layer is adsorbed on the surface of the material. As most adsorption processes (except chemisorption) don't follow this behaviour, it is important to regard the Langmuir surface area as an estimate.

As with the BET area, the Langmuir area is calculated by using the code in Listing 1.4. The framework will alert the user if the correlation is not linear in the selected range. Here the `verbose=True` option prints a short text with all the calculation variables and the Langmuir plot as seen in Figure 1.3a. If desired the user can override automatic pressure range selection as seen in the bottom of Listing 1.4.

Listing 1.4: Calculating a Langmuir area

```
1 area_dict = pygaps.area_langmuir(isotherm, verbose=True)

| WARNING The correlation is not linear!

1 area_dict = pygaps.area_langmuir(isotherm,
2                                 limits=(0.05, 0.3),
3                                 verbose=True)

| Langmuir surface area:  a = 415 m2/g
| Minimum pressure point chosen is 0.0 and maximum is 0.194
| The slope of the Langmuir line:      s = 234.968
| The intercept of the Langmuir line:  i = 1.607
| The Langmuir constant is:           K = 146
| Amount for a monolayer:             n = 0.00426 mol/g
```

## Ideal isotherms or thickness functions

The initial part of an isotherm (the Henry regime) can be seen to be very dependent on the interactions between the adsorbate and the surface. However, the subsequent layers are less influenced by the initial layer and can often be assumed, like in the BET model, to have an energy of adsorption identical to the enthalpy of liquefaction of the bulk liquid and whose formation depends essentially only on the partial pressure.

With this assumption, several studies have been focused on obtaining a reference isotherm for adsorption on a non-porous material which can then, if the cross-sectional

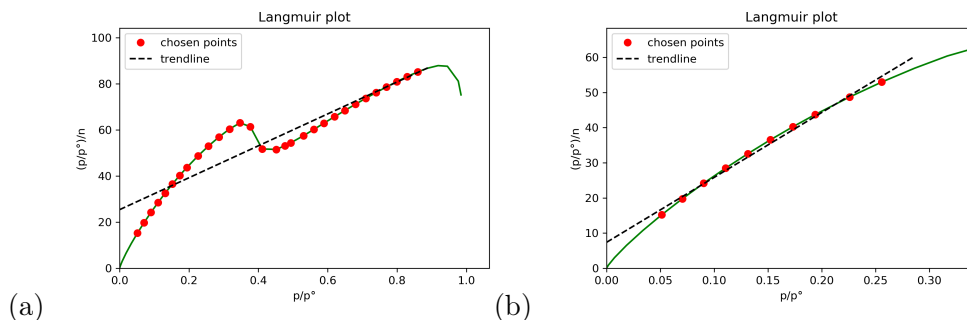


Figure 1.3: Output from the Langmuir area function (a) the Langmuir plot showing the automatic fitting attempt which generates a warning and (b) a manually selected pressure range for the Langmuir plot.

area of the molecule is known, be transformed in a function capable of predicting the multilayer adsorbate thickness as a function of pressure. This empirical function, also referred to as a *thickness function* or *t-curve*, can then be used as an alternative method for surface area determination, as explained in the next section. These curves are also used in the classical methods for calculating mesoporous size distributions. It is important to clarify that the function is only applicable for a single adsorbent and a single temperature.

Several common thickness functions have been implemented in **pyGAPS**, applicable for nitrogen at 77 K such as the Halsey<sup>(18)</sup> (equation 1.34) and the Harkins and Jura<sup>(19)</sup> (equation 1.35) curves.

$$t_{Halsey} = 0.354 \left( \frac{-5}{\log(p/p_0)} \right)^{1/3} \quad (1.34)$$

$$t_{Harkins\&Jura} = \left( \frac{0.1399}{0.034 - \log_{10}(p/p_0)} \right)^{1/2} \quad (1.35)$$

These t-curves are selected by name as parameters in the functions that use them. The user can also define their own t-curve as a function and pass it as a parameter. An example is shown in Listing ?? in the t-plot section.

## t-plot Method

The t-plot method is an empirical method, developed as a tool to determine the surface area of porous materials, which can also be used for other calculations, such as external pore area and micropore volume calculations.<sup>(20)</sup> A plot is constructed, where the isotherm loading data is plotted versus the ideal thickness of the adsorbate layer, obtained through the a t-curve (1.3.2). It stands to reason that, in the case when the experimentally measured loading follows the model, a straight line will be obtained with its intercept through the origin. However, since in most cases there are differences be-

check  
equa-  
tions

tween adsorption in the pores and ideal surface adsorption, the t-plot will deviate and form features which can be analysed to describe the material characteristics.

- A sharp vertical deviation will indicate condensation in a type of pore.
- A gradual slope will indicate adsorption on the wall of a particular pore.

The slope of the linear section can be used to calculate the area where the adsorption is taking place. If it is of a linear region at the start of the curve, it will represent the total surface area of the material. If at the end of the curve, it will instead represent external surface area of the sample. The formula to calculate the area is where  $\rho_l$  is the liquid density of the adsorbate at experimental conditions

$$A = \frac{sM_m}{\rho_l} \quad (1.36)$$

If the region selected is after a vertical deviation, the intercept of the line will no longer pass through the origin. This intercept be used to calculate the pore volume through the following equation:

$$V_{ads} = \frac{iM_m}{\rho_l} \quad (1.37)$$

Since the t-plot method is representing a difference between the isotherm and a model, care must be taken to ensure that the model actually describes the thickness of a layer of adsorbate on the surface of the adsorbent. This is more difficult than it appears as no universal thickness curve exists. When selecting a thickness model, make sure that it is applicable to both the material and the adsorbate. Interactions at loadings that occur on the t-plot lower than the monolayer thickness do not have any physical meaning.

When the function is called without any other parameters, the framework will attempt to find plateaus in the data and automatically fit them with a straight line, returning a dictionary with the slope, intercept and calculated pore volume and specific area for each region fitted. As an example, the first function in Listing 1.5 will generate the graph in Figure 1.4a. The isotherm in this example is measured on a sample of MCM-41.

Listing 1.5: Generating a t-plot

```

1 # using automatic region detection
2 pygaps.t_plot(isotherm, verbose=True)
3
4 # specifying a manual region
5 pygaps.t_plot(isotherm, limits=(0.3,0.44), verbose=True)
6
7 # using the Halsey thickness curve
8 pygaps.t_plot(isotherm, thickness_model='Halsey', verbose=True)
9
10 # defining a custom t-curve to use in the t-plot

```

```

11 def carbon_model(relative_p):
12     return 0.88*(relative_p**2) + 6.45*relative_p + 2.98
13
14 pygaps.t_plot(isotherm, thickness_model=carbon_model, verbose=True)

```

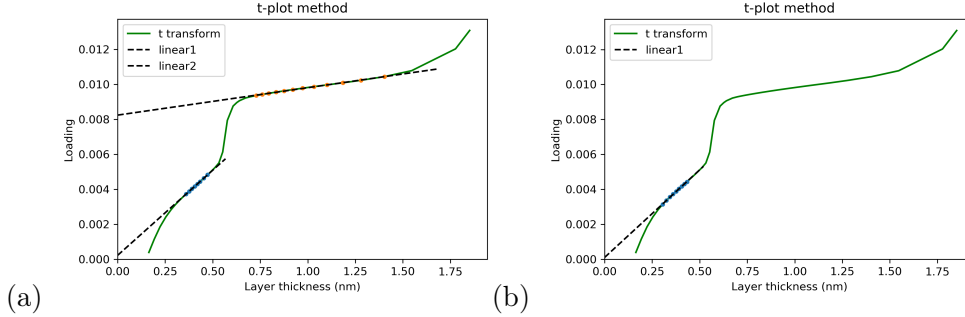


Figure 1.4: Output from the t-plot method function (a) an automatically obtained t-plot with the calculated fit regions and (b) a manually selected range for the t-plot.

The first line in Figure 1.4a can be attributed to adsorption on the pore surface, while the second one is adsorption on the external surface after mesopore filling. Two values are calculated for each section detected: the adsorbed volume and the corresponding surface area. In this case, the area of the first linear region corresponds to the mesopore area.

We can obtain a more accurate result for the surface area by fitting the first linear region to a zero intercept by using the manual region selection. Finally, the framework allows for the thickness model to be substituted with an user-provided function which will be used for the thickness calculation, as mentioned in the t-curve section (1.3.2). A carbon black-type thickness curve is used here.

### $\alpha_s$ Method

In order to extend the t-plot analysis with other adsorbents and non-standard thickness curves, the  $\alpha_s$  method was devised.<sup>(21)</sup> Instead of attempting to find an ideal isotherm that describes the thickness of the adsorbed layer, a reference isotherm is used. This isotherm is measured on a non-porous version of the material, with the same surface characteristics and with the same gas. The dimensionless  $\alpha_s$  values are obtained from this isotherm by dividing the loading values by the amount adsorbed at a specific relative pressure, usually taken as 0.4 as nitrogen hysteresis loops theoretically close at this value.

$$\alpha_s = \frac{n_a}{n_{0.4}} \quad (1.38)$$

The analysis then proceeds as in the t-plot method. The slope of the linear section can be used to calculate the area where the adsorption is taking place. If it is of a linear



region at the start of the curve, it will represent the total surface area of the material. If at the end of the curve, it will instead represent external surface area of the sample. The calculation uses the known area of the reference material.

$$A = \frac{sA_{ref}}{(n_{ref})_{0.4}} \quad (1.39)$$

If the region selected is after a vertical deviation, the intercept of the line will no longer pass through the origin. This intercept be used to calculate the pore volume through the following equation:

$$V_{ads} = \frac{iM_m}{\rho_l} \quad (1.40)$$

The reference isotherm chosen for the  $\alpha_s$  method must be a description of the adsorption on a completely non-porous sample of the same material. It is often impossible to obtain such non-porous versions, therefore care must be taken how the reference isotherm is defined.

To generate an  $\alpha_s$ -plot in `pyGAPS`, both an analysis isotherm and a reference isotherm must be supplied as shown in Listing 1.6. In this example, the reference isotherm is measured on non-porous silica. The reference material area can be specified by using the `reference_area` parameter. If not specified, it is automatically calculated by applying the BET method on the reference isotherm.

Listing 1.6: Generating an  $\alpha_s$ -plot

```
1 pygaps.alpha_s(isotherm,
2               reference_isotherm=isotherm_r,
3               verbose=True)
```

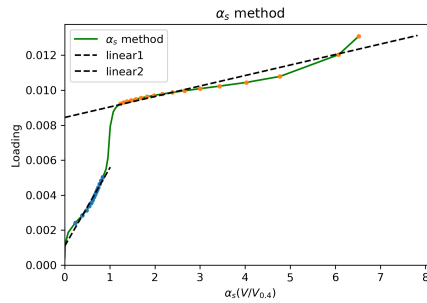


Figure 1.5: Output from the  $\alpha_s$ -plot function showing two automatically fit regions.

### 1.3.3 Assessing porosity

Characterization of pore sizes and their distribution in porous materials is often the main goal when performing adsorption experiments. It is therefore important that `pyGAPS` includes several robust methods for determining pore distribution from isotherm data.

When it comes to porous materials, three kinds of pore sizes have been defined, based on their lengthscales: micropores ( $<2$  nm), mesopores (2 nm to 50 nm), and macropores ( $>50$  nm).

Macropores are generally unable to be characterised through adsorption, with methods such as mercury intrusion porosimetry as the standard for pore size distributions in this lengthscale, although other alternatives have been suggested<sup>(22)</sup> due to the high toxicity of mercury. Therefore, they are outside the scope of this framework.

In the mesopore range, the “classical” methods are usually applied, based on the application of Kelvin’s equation pertaining to capillary condensation. This equation calculates the critical pressure at which the fluid completely files a pore of a specific length. This equation, applicable to a range of geometries, is used in multiple approaches such as the original Barrett-Joyner-Halenda (BJH) method or the Dollimore-Heal (DH) method.

For microporous materials, the Kelvin equation with its assumptions of continuous fluid properties and equal density of the adsorbed state to bulk liquid density breaks down. An atomistic approach is required here, to address the interaction between solid-fluid and fluid-fluid through potential functions. The Horvath-Kawazoe or HK method is often used, and it is implemented in `pyGAPS`.

Finally, methods based on density functional theory (DFT) and similar variants such as non-local DFT (NLDF) and quenched solid state DFT (QSDFT) should be mentioned, as they can be used for multiscale (micropore and mesopore) characterisation. These methods rely on the *in-silico* simulation of isotherms on a range of pore sizes, which can then be collated in a so-called *kernel* able to be used in decomposition of a experimental isotherm to obtain a pore size distribution. While the generation of DFT kernels is outside the scope of the `pyGAPS` framework, it is able to use user-provided kernels to fit adsorption isotherms, and comes with a basic kernel for  $N_2$  adsorption at 77 K on carbon slit pores.

It should be noted that all methods described require knowledge of the pore geometry as well as depend on the material having pores which conform to this well-defined shape. Real adsorbents usually have interconnected networks of irregular pores, which may only be approximated by the ideal pores used in these models.

### Mesoporous size distribution

**The Kelvin equation** Since the Kelvin equation is the basis of both the BJH and DH methods its theory and its implementation will be described here.

According to Rouquerol,<sup>(7)</sup> in adopting this approach, it is assumed that:

- The Kelvin equation is applicable over the pore range (mesopores). Therefore in pores which are below a certain size (around 2.5 nm), the granularity of the liquid-vapour interface becomes too large for classical bulk methods to be applied.
- The meniscus curvature is controlled by the pore size and shape. Ideal shapes for the curvature are assumed.

- The pores are rigid and of well defined shape. They are considered open-ended and non-intersecting
- The filling/emptying of each pore does not depend on its location.
- The adsorption on the pore walls is not different from surface adsorption.

The Kelvin equation assumes that adsorption in a pore is not different than adsorption on a standard surface. Therefore, no interactions with the adsorbent is accounted for. Furthermore, the geometry of the pore itself is considered to be invariant across the entire adsorbate.

**Barrett, Joyner and Halenda (BJH) pore size distribution** Calculates the pore size distribution using a *classical* model which attempts to describe the adsorption in a pore as a combination of a statistical thickness and a condensation/evaporation behaviour described by surface tension

The BJH method for calculating pore size distribution is based on a classical description of the adsorbate behaviour in the adsorbent pores.<sup>(1)</sup> Under this method, the adsorbate is adsorbing on the pore walls in a predictable way, and decreasing the apparent pore volume until condensation takes place, filling the entire pore. The critical radius is a sum of two radii, the adsorbed layer thickness, which can be modelled by a thickness model (such as Halsey, Harkins & Jura as presented in Section 1.3.2) and a critical radius model for condensation/evaporation, based on a form of the Kelvin equation.

$$r_p = t + r_k \quad (1.41)$$

The original model used the desorption curve as a basis for calculating pore size distribution. Between two points of the curve, the volume desorbed can be described as the volume contribution from pore evaporation and the volume from layer thickness decrease as per the equation above. The computation is done cumulatively, starting from the filled pores and calculating for each point the volume adsorbed in a pore from the following equation:

$$V_p = \left( \frac{\bar{r}_p}{\bar{r}_k + \Delta t_n} \right)^2 \left( \Delta V_n - \Delta t_n \sum_{i=1}^{n-1} \Delta A_p + \Delta t_n \bar{t}_n \sum_{i=1}^{n-1} \frac{\Delta A_p}{\bar{r}_p} \right) \quad (1.42)$$

$$A = 2\Delta V_p / r_p \quad (1.43)$$

Where:

- $\Delta A_p$  is the area of the pores
- $\Delta V_p$  is the adsorbed volume change between two points

- $\bar{r}_p$  is the average pore radius calculated as a sum of the kelvin radius and layer thickness of the pores at pressure p between two measurement points
- $\bar{r}_k$  is the average kelvin radius between two measurement points
- $\bar{t}_n$  is the average layer thickness between two measurement points
- $\Delta t_n$  is the average change in layer thickness between two measurement points

Then, by plotting  $\Delta V/(2 * \Delta r_p)$  versus the width of the pores calculated for each point, the pore size distribution can be obtained.

**Dollimore-Heal pore size distribution** The DH or Dollimore-Heal method<sup>(23)</sup> of calculation of pore size distribution is an extension of the BJH method, which takes into account the geometry of the pores by introducing a length component.

Like the BJH method, it is based on a classical description of the adsorbate behaviour in the adsorbent pores.

$$V_p = \left( \frac{\bar{r}_p}{\bar{r}_k + \Delta t_n} \right)^2 \left( \Delta V_n - \Delta t_n \sum_{i=1}^{n-1} \Delta A_p + 2\pi \Delta t_n \bar{t}_n \sum_{i=1}^{n-1} L_p \right) \quad (1.44)$$

$$A = 2\Delta V_p / r_p \quad (1.45)$$

$$L = \Delta A_p / 2\pi r_p \quad (1.46)$$

Where:

- $\Delta A_p$  is the area of the pores
- $\Delta V_p$  is the adsorbed volume change between two points
- $\bar{r}_p$  is the average pore radius calculated as a sum of the kelvin radius and layer thickness of the pores at pressure p between two measurement points
- $\bar{r}_k$  is the average kelvin radius between two measurement points
- $\bar{t}_n$  is the average layer thickness between two measurement points
- $\Delta t_n$  is the average change in layer thickness between two measurement points

Then, by plotting  $\Delta V/(2 * \Delta r_p)$  versus the width of the pores calculated for each point, the pore size distribution can be obtained.

### Microporous size distribution

The H-K method attempts to describe the adsorption within pores by calculation of the average potential energy for a pore.<sup>(24)</sup> The method starts by assuming the relationship between the gas phase as being:

$$R_g T \ln\left(\frac{p}{p_0}\right) = U_0 + P_a \quad (1.47)$$

Here  $U_0$  is the potential function describing the surface to adsorbent interactions and  $P_a$  is the potential function describing the adsorbate- adsorbate interactions. This equation is derived from the equation of the free energy of adsorption at constant temperature where term  $T\Delta S^{tr}(w/w_\infty)$  is assumed to be negligible.

If a Lennard-Jones-type potential function describes the interactions between the adsorbate molecules and the adsorbent molecules then the two contributions to the total potential can be replaced by the extended function. The resulting equation becomes

$$RT \ln(p/p_0) = N_A \frac{n_a A_a + n_A A_A}{2\sigma^4(l-d)} \times \int_{d/2}^{1-d/2} \left[ -\left(\frac{\sigma}{r}\right)^4 + \left(\frac{\sigma}{r}\right)^{10} - \left(\frac{\sigma}{l-r}\right)^4 + \left(\frac{\sigma}{l-r}\right)^4 \right] dx \quad (1.48)$$

where  $l$  is the width of the pore,  $d$  defined as  $d = d_a + d_A$  is the sum of the diameters of the adsorbate and adsorbent molecules,  $n_a$  is number of molecules of adsorbent and  $A_a$  and  $A_A$  the Lennard-Jones potential constant of the fluid molecule and solid molecule respectively which are defined as

$$A_a = \frac{6mc^2\alpha_a\alpha_A}{\alpha_a/\chi_a + \alpha_A/\chi_A} \quad (1.49)$$

and

$$A_a = \frac{3mc^2\alpha_A\chi_A}{2} \quad (1.50)$$

Here  $m$  is the mass of an electron,  $\alpha_a$  and  $\alpha_A$  are the polarizability of the adsorbate and adsorbate molecule and  $\chi_a$  and  $\chi_A$  the magnetic susceptibility of the adsorbate molecule and adsorbent molecule, respectively.

The HK method is applicable to slit pores, and it can be modified to be extended to cylindrical and spherical pores. It is worth noting that there are several assumptions made which limit its applicability:

- It does not have a description of capillary condensation. This means that the pore size distribution can only be considered accurate up to a maximum of 5 nm.

- Each pore is modelled as uniform and of infinite length. Materials with varying pore shapes or highly interconnected networks may not give realistic results.
- The HK method is reliant on knowledge of the properties of the surface atoms. This assumption is true only if the material surface is homogenous. Furthermore, longer range interactions with multiple surface layers are not considered.
- Only dispersive forces are accounted for. If the adsorbate-adsorbent interactions have other specific contributions, the Lennard-Jones potential function will not be an accurate description of pore environment.

The `pyGAPS` framework contains the required physical properties for the most commonly used adsorbates, as well as properties from literature for several materials: the original parameters developed by Horvath and Kawazoe for a carbon surface <sup>(24)</sup> and the oxide surface parameters published by Saito and Foley. <sup>(25)</sup> The user can provide custom dictionary of these parameters when calling the function.

Listing 1.7: Using the HK method for PSD

```
# Calling the HK micropore method with the
# Saito-Foley oxide surface parameters
result_dict = pygaps.micropore_size_distribution(
    isotherm ,
    psd_model='HK' ,
    adsorbent_model='OxideIon(SF)' ,
    verbose=True
)
# Defining a custom adsorbate parameter dictionary
# and using it in the HK method
adsorbate_params = {
    'magnetic_susceptibility': 3.6e-35,
    'molecular_diameter': 0.3,
    'polarizability': 1.76e-30,
    'surface_density': 6.71e+18
}
result_dict = pygaps.micropore_size_distribution(
    isotherm ,
    psd_model='HK' ,
    adsorbent_model='OxideIon(SF)' ,
    adsorbate_model=adsorbate_params ,
    verbose=True
)
```

## DFT kernel fitting

The function will take the data in the form of pressure and loading. It will then load the kernel either from disk or from memory and define a minimization function as the sum

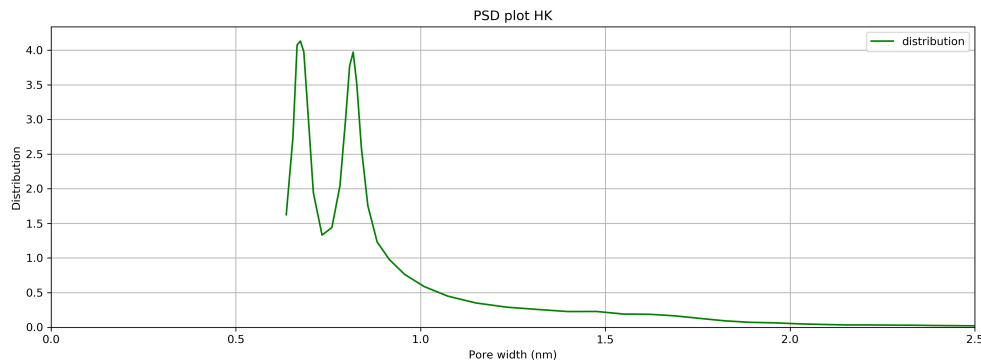


Figure 1.6: Pore size distribution calculated through the Horvath-Kawazoe method

of squared differences of the sum of all individual kernel isotherm loadings multiplied by their contribution as per the following function:

$$f(x) = \sum_{p=p_0}^{p=p_x} (n_{p,exp} - \sum_{w=w_0}^{w=w_y} n_{p,kernel} X_w)^2 \quad (1.51)$$

## 1.4 Case studies

### 1.4.1 Routine characterization of a MOF sample

When a newly synthesised sample is available, an initial characterisation is often performed to compare the material with previous batches. Adsorption of nitrogen at 77 K is commonly used to verify if predictors such as specific surface area and pore size distribution are consistent with other samples or literature values.

The nitrogen isotherm is first imported in `pyGAPS`. To obtain the BET area, the `pygaps.area_BET()` method is used with the isotherm object as the parameter and the verbose option, with Figure 1.7 as the output. It can be seen that the framework has automatically selected the points within the applicable BET region using the checks devised by Rouquerol et al.<sup>(7)</sup> to assert method validity. The statistical BET monolayer point is within the selected region, which is one of the checks implemented for method validity. The calculated surface area is 1277 m<sup>2</sup>/g, which is similar to literature values.<sup>(26,27)</sup>

The same isotherm is used to calculate the pore size distribution of the UiO-66(Zr) sample. This MOF has octahedral cages surrounded by eight corner tetrahedral cages of 11 and 8 Å respectively. The structure is therefore expected to have only micropores. Two methods are available in `pyGAPS` for micropore size distributions: a ‘classical’ Horvath-Kawazoe (HK) method,<sup>(24)</sup> as well as a DFT fitting routine. The HK method is called by using the function in Listing 1.8. Here, the surface characteristic parameters determined by Saito and Foley<sup>(25)</sup> are to be used, with the framework automatically

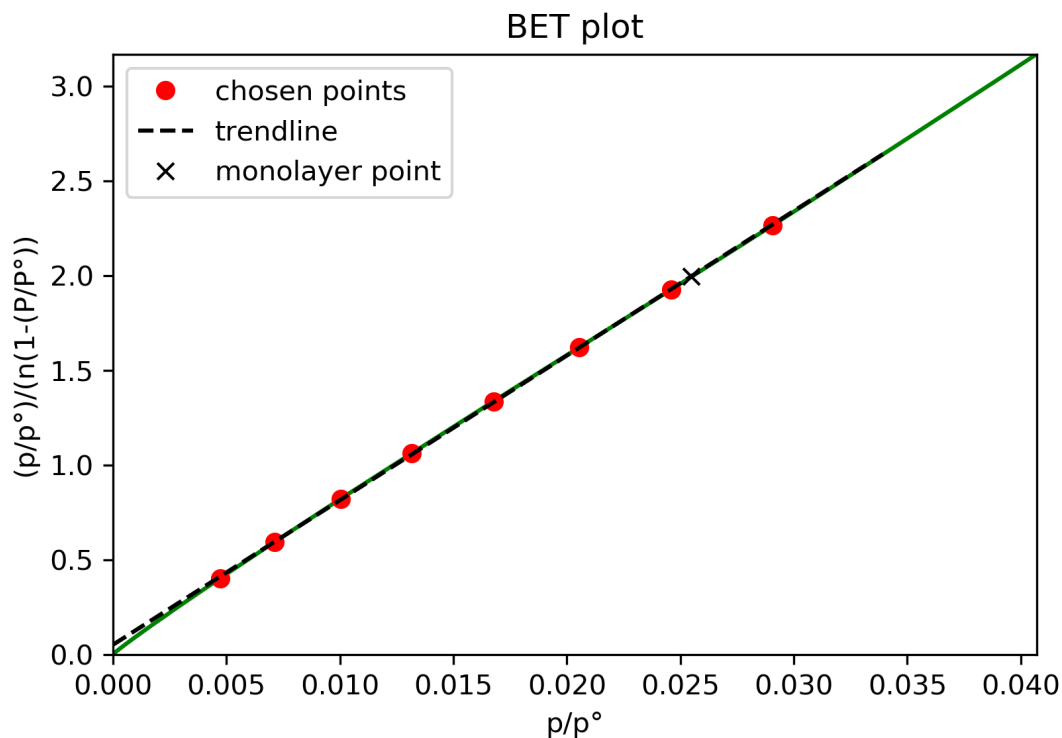


Figure 1.7: BET transformation and point selection

supplying the parameters for the adsorbed gas.

Listing 1.8: Calculating the PSD

```
pygaps.micropore_size_distribution(iso ,
                                   psd_model='HK' ,
                                   adsorbent_model='OxideIon(SF)')
pygaps.dft_size_distribution(iso , kernel_path='internal')
```

The DFT fitting is done using the internal kernel which is applicable for  $N_2$  on carbon slit pores and included with pyGAPS. Results are shown in Figure 1.8. We can see that whilst both methods produce a bimodal size distribution, neither is accurate in describing the crystallographic pore widths. This is to be expected, since neither method is applicable to the UiO-66(Zr) system. However, when comparing two samples of the same MOF, these methods can still highlight differences in the quality of the two batches. For example, it can be seen that the DFT method shows wide peaks at  $>1$  nm which can be an indication of the presence of defects in the UiO-66(Zr) structure. Indeed, TGA analysis of the pristine sample shows a linker ratio (11.8 linkers per cluster) that is lower than it would be in a perfect sample (see figure in supplemental information.)

New materials are often screened for their ability to act as a  $CO_2$  capture material. A good predictor of performance in this application are the enthalpies of adsorption, which are an indication of host-guest interactions. Here, we first measure the differential heats



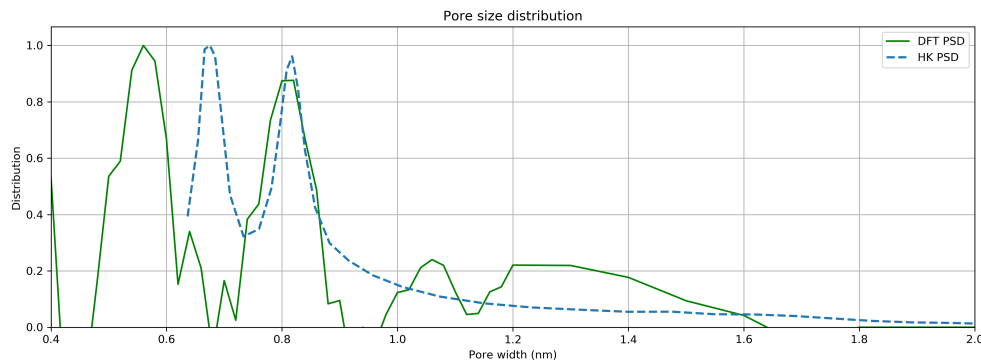


Figure 1.8: Pore size distribution calculated through the Horvath-Kawazoe method (dotted blue line) and the internal DFT kernel (continuous green line)

of adsorption directly through the use of adsorption microcalorimetry at 303 K. Then, to determine the isosteric heats of adsorption, two isotherms have been measured at 303 K and 323 K respectively. The complete set of isotherms is loaded into `pyGAPS` and plotted by the `pygaps.plot_iso()` function as seen in Figure 1.9a. To calculate the isosteric heat of adsorption, the two isotherms measured for this purpose are passed through the `pygaps.isosteric_heat()` function. The results from the calculation are overlaid on top of the measured calorimetric data in Figure 1.9b. The two datasets are overlap for the most part but diverge at low loadings and near complete coverage. At low loading the small changes in pressure amount introduce large errors in the Clausius-Clapeyron equation. This, together with the breakdown of the assumption of equilibrium due to active sites in the MOF lead to the calorimetric measurement providing more valid results. At higher loadings, where the isotherm reaches a plateau and the change in adsorbed amount is small from point to point, errors are introduced in the direct calculation of the heat of adsorption. The two techniques are thus complementary.

### 1.4.2 Analysis of a carbon sample for gas separation applications

A sample of reference carbon Takeda 5A is to be investigated for an in-depth characterisation of the adsorption behaviour of pure gases, with a focus on describing the pore environment. Afterwards, the performance of different binary separations is evaluated, such as  $\text{CO}_2/\text{N}_2$  and propane/propylene.

Pure gas adsorption data has been recorded at 303 K in conjunction with microcalorimetry on  $\text{N}_2$ ,  $\text{CO}$ ,  $\text{CO}_2$ ,  $\text{CH}_4$ ,  $\text{C}_2\text{H}_6$ ,  $\text{C}_3\text{H}_6$  and  $\text{C}_3\text{H}_8$ . The complete dataset is plotted with the `pygaps.plot_iso()` function and can be seen in Figure 1.10a.

Nitrogen and carbon monoxide are similar in their adsorption behaviour, with a nearly linear isotherm and low capacities. Hydrocarbons are adsorbed with higher loadings, with both propane and propylene reaching a plateau at low pressures. Propylene is seen to have a higher capacity than propane, with packing effects as a likely cause. Carbon dioxide has the highest loading capacity of the entire dataset.

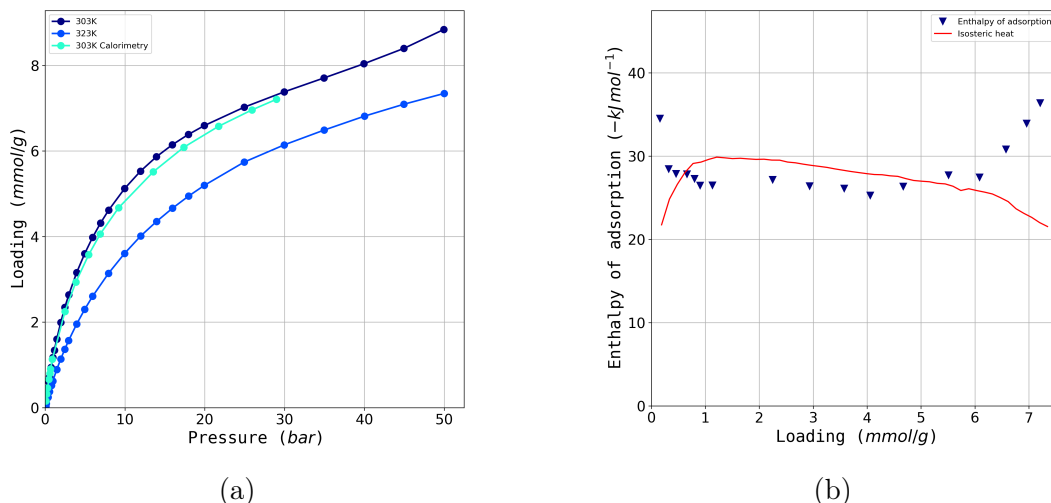


Figure 1.9: Calculation of enthalpy of adsorption: (a) the dataset of isotherms used and (b) the calculated isosteric heat (red line) together with the measured differential enthalpy of adsorption (blue triangles)

Two parameters can be useful in characterising the local pore environment before guest-guest interactions come into effect: the Henry constant at low loadings as well as the initial enthalpy of adsorption. Both can be calculated with `pyGAPS`, with several options in regard to the methodology. Here, Henry’s constant is calculated using the `pygaps.initial_henry_virial()` function, which fits a virial model to the isotherm and then takes the limit at loading approaching zero. The initial enthalpy of adsorption is obtained through the `pygaps.initial_enthalpy_comp()` function. This fits the enthalpy curve to a compound contribution from guest-host interaction, defects, guest-guest attraction and repulsion using a minimization algorithm. The results of the calculations are plotted versus the polarizability of the gas used, which can be obtained from the respective `Adsorbate` class. Figure 1.10b shows that both the parameters fall on a linear trend, which suggests that the interactions between those guests and the pore walls are mostly due to Lennard-Jones interactions. Carbon dioxide has a higher enthalpy of adsorption than the baseline due to the contribution from its quadrupole moment. There is almost a complete overlap between propane and propylene, which leads to the conclusion that the unsaturated double bond does not interact in a specific way with the carbon surface. The difference between the two isotherms is due exclusively to steric and packing effects.

From the analysis of the pure gas dataset and the property-polarizability graph, two potentially interesting separations arise, namely  $CO_2-N_2$  and propylene-propane. For these two pairs we use ideal adsorbed solution theory (IAST) to simulate binary adsorption behaviour. The `pyGAPS` framework includes a modified version of the `pyIAST` code<sup>(28)</sup> which has been adapted to work with the `Isotherm` classes. Both model isotherms and real data can be used for IAST, with spreading pressure being calculated through the underlying isotherm model or through interpolation, respectively. Based

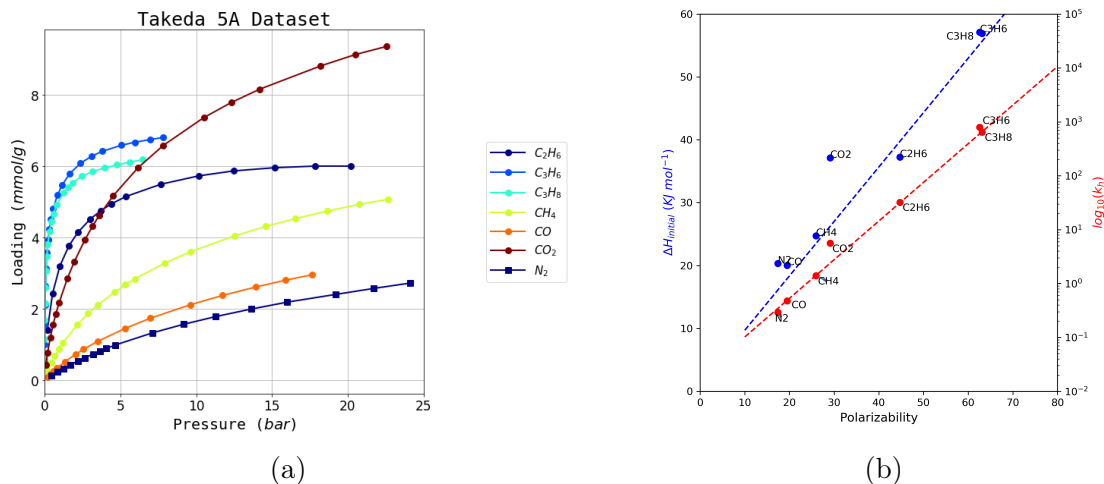


Figure 1.10: Takeda 5A dataset processing: (a) the experimental dataset all recorded gases and (b) the calculated trends of initial heat of adsorption and Henry's constant

on the previous analysis, we expect to see good performance for carbon dioxide capture and little or no selectivity in the paraffin-olefin pair.

In this case, we fit the experimental data to the available models in `pyGAPS`, then use the resulting model isotherms for IAST simulations. In order to get a 'best-fit' model isotherm, we use the function in Listing 1.9, which fits all available models and selects the one with the lowest residuals between the fitted function and the real data. Currently, the models available in `pyGAPS` are: Henry, single, double and triple site Langmuir,<sup>(8)</sup> BET,<sup>(9)</sup> Quadratic,<sup>(13)</sup> Jensen-Seaton,<sup>(12)</sup> Toth,<sup>(29)</sup> Temptkin approximation,<sup>(11)</sup> Virial,<sup>(14)</sup> and the Flory-Huggins<sup>(16)</sup> and Wilson<sup>(15)</sup> variations of Vacancy Solution Theory (VST). The isotherms and their best-fitting model is displayed in Figure 1.11a for the  $CO_2$ - $N_2$  pair and in Figure 1.12a for the  $C_3H_8$ - $C_3H_6$  pair.

Listing 1.9: Guessing the best model

```
model = pygaps.ModelIsotherm.from_pointisotherm(iso, guess_model=True)
```

For the carbon dioxide separation, we simulate all equilibrium points for the adsorbed and gaseous phases at different concentrations of the two gases at 1 bar. To do this we use the `pygaps.iast_vle()` function which produces an analogue of a vapour-liquid equilibrium at a specified pressure for a binary mixture. The resulting graph of this function can be seen in Figure 1.12b. As expected, the predicted adsorbed mixture is rich in carbon dioxide. Selectivity can also be calculated in a single point, with the value at 15%  $CO_2$  and 1 bar being 16.5.

For the propane-propylene separation, we simulate the selectivity for propane within a pressure range for a 50% mixture of the two gases. It can be seen that there is little or no preference for the unsaturated molecule, though the selectivity increases slightly at pressures above 1 bar.

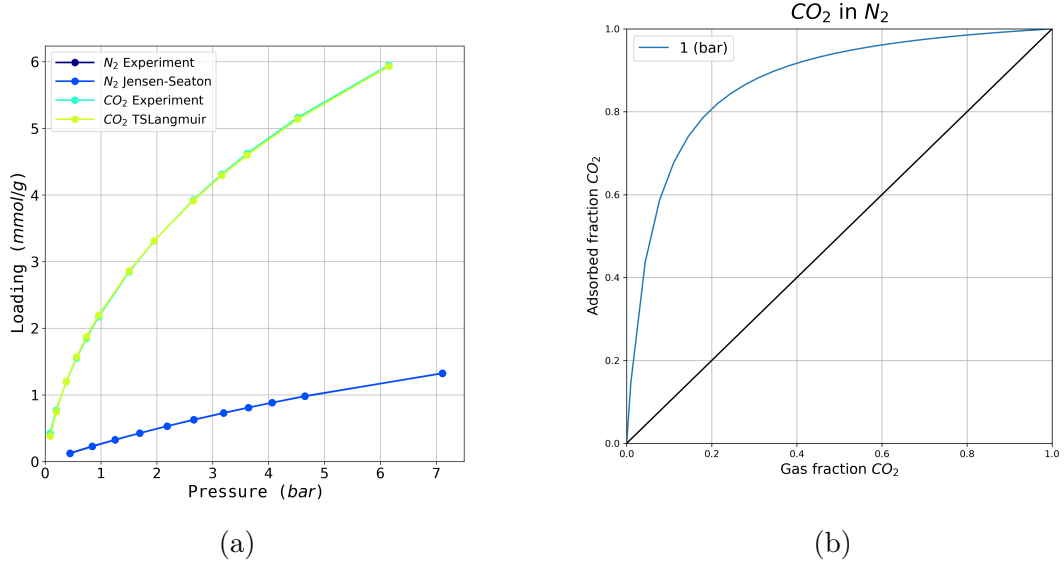


Figure 1.11: Modelling binary adsorption of  $CO_2$  and  $N_2$ : (a) the pure component isotherms and their best fit models and (b) the predicted composition of the gaseous and adsorbed phase for different fractions of  $CO_2$  at 1 bar

## 1.5 Conclusion

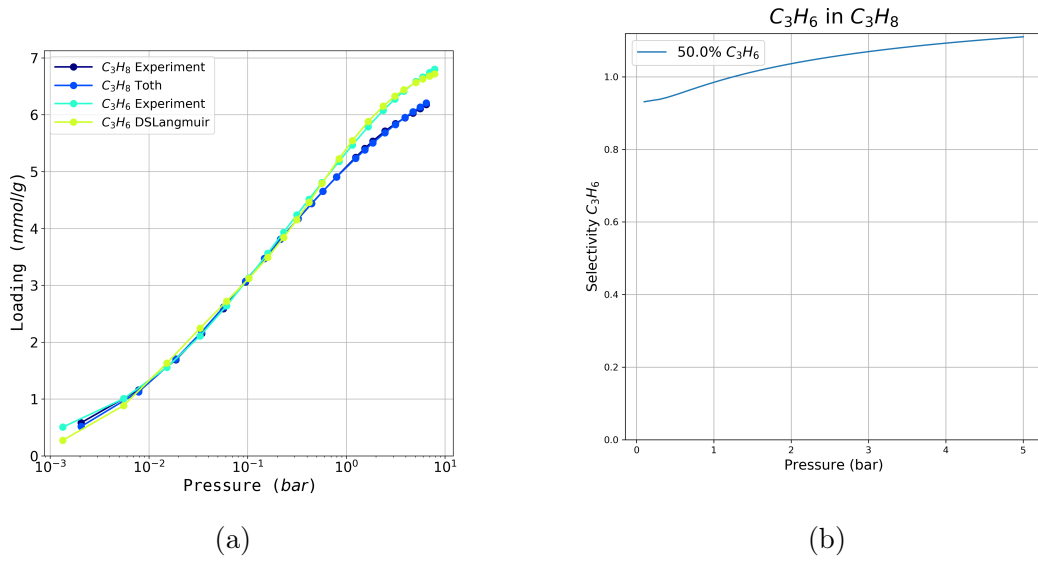


Figure 1.12: Modelling binary adsorption of a propane-propylene mixture: (a) the pure-component isotherms and their best fit models and (b) the predicted selectivity of propane adsorption of a 50-50% mixture in a range of pressure from 0.1 to 7 bar

# Bibliography

- [1] Elliott P. Barrett, Leslie G. Joyner, and Paul P. Halenda. The Determination of Pore Volume and Area Distributions in Porous Substances. I. Computations from Nitrogen Isotherms. *Journal of the American Chemical Society*, 73(1):373–380, January 1951. ISSN 0002-7863. doi: 10.1021/ja01145a126.
- [2] N.A. Seaton, J.P.R.B. Walton, and N. Quirke. A new analysis method for the determination of the pore size distribution of porous carbons from nitrogen adsorption measurements. *Carbon*, 27(6):853–861, 1989. ISSN 00086223. doi: 10.1016/0008-6223(89)90035-3.
- [3] P. Tarazona, U. Marini Bettolo Marconi, and R. Evans. Phase equilibria of fluid interfaces and confined fluids: Non-local versus local density functionals. *Molecular Physics*, 60(3):573–595, February 1987. ISSN 0026-8976, 1362-3028. doi: 10.1080/00268978700100381.
- [4] Dan Siderius, Vincent Shen, and Russell Johnson. NIST / ARPA-E Database of Novel and Emerging Adsorbent Materials, NIST Standard Reference Database 205, 2015.
- [5] Ian H. Bell, Jorrit Wronski, Sylvain Quoilin, and Vincent Lemort. Pure and Pseudo-pure Fluid Thermophysical Property Evaluation and the Open-Source Thermophysical Property Library CoolProp. *Industrial & Engineering Chemistry Research*, 53(6):2498–2508, February 2014. ISSN 0888-5885, 1520-5045. doi: 10.1021/ie4033999.
- [6] Eric Lemmon. NIST Reference Fluid Thermodynamic and Transport Properties Database: Version 9.0, NIST Standard Reference Database 23, 1989.
- [7] Jean Rouquerol, Françoise Rouquerol, Philip L. Llewellyn, Guillaume Maurin, and Kenneth Sing. *Adsorption by Powders and Porous Solids : Principles, Methodology and Applications*. 2013. ISBN 978-0-08-097035-6.
- [8] Irving Langmuir. The Adsorption of Gases on Plane Surfaces of Glass, Mica and Platinum. *Journal of the American Chemical Society*, 40(9):1361–1403, September 1918. ISSN 0002-7863, 1520-5126. doi: 10.1021/ja02242a004.
- [9] Stephen Brunauer, P. H. Emmett, and Edward Teller. Adsorption of Gases in Multimolecular Layers. *Journal of the American Chemical Society*, 60(2):309–319, February 1938. ISSN 0002-7863, 1520-5126. doi: 10.1021/ja01269a023.
- [10] Mikhail Temkin. Kinetics of ammonia synthesis on promoted iron catalyst. *Acta Phys. Chim. USSR*, 12:327–356, 1940.

## Bibliography

- [11] Cory M. Simon, Jihan Kim, Li-Chiang Lin, Richard L. Martin, Maciej Haranczyk, and Berend Smit. Optimizing nanoporous materials for gas storage. *Physical Chemistry Chemical Physics*, 16(12):5499, 2014. ISSN 1463-9076, 1463-9084. doi: 10.1039/c3cp55039g.
- [12] C. R. C. Jensen and N. A. Seaton. An isotherm equation for adsorption to high pressures in microporous adsorbents. *Langmuir*, 12(11):2866–2867, 1996.
- [13] Terrell L. Hill. *An Introduction to Statistical Thermodynamics*. Dover Publications, New York, 1986. ISBN 978-0-486-65242-9.
- [14] Alan L. Myers. Thermodynamics of adsorption in porous materials. *AIChE Journal*, 48(1):145–160, January 2002. ISSN 00011541. doi: 10.1002/aic.690480115.
- [15] Solot Suwanayuen and Ronald P. Danner. A gas adsorption isotherm equation based on vacancy solution theory. *AIChE Journal*, 26(1):68–76, January 1980. ISSN 00011541. doi: 10.1002/aic.690260112.
- [16] T. W. Cochran, R. L. Kabel, and R. P. Danner. Vacancy solution theory of adsorption using Flory-Huggins activity coefficient equations. *AIChE Journal*, 31(2): 268–277, February 1985. ISSN 0001-1541, 1547-5905. doi: 10.1002/aic.690310214.
- [17] Matthias Thommes, Katsumi Kaneko, Alexander V. Neimark, James P. Olivier, Francisco Rodriguez-Reinoso, Jean Rouquerol, and Kenneth S W Sing. Physisorption of gases, with special reference to the evaluation of surface area and pore size distribution (IUPAC Technical Report). *Pure and Applied Chemistry*, 87(9-10): 1051–1069, 2015. ISSN 13653075. doi: 10.1515/pac-2014-1117.
- [18] George Halsey. Physical Adsorption on Non-Uniform Surfaces. *The Journal of Chemical Physics*, 16(10):931–937, October 1948. ISSN 0021-9606, 1089-7690. doi: 10.1063/1.1746689.
- [19] William D. Harkins and George Jura. Surfaces of Solids. XIII. A Vapor Adsorption Method for the Determination of the Area of a Solid without the Assumption of a Molecular Area, and the Areas Occupied by Nitrogen and Other Molecules on the Surface of a Solid. *Journal of the American Chemical Society*, 66(8):1366–1373, August 1944. ISSN 0002-7863, 1520-5126. doi: 10.1021/ja01236a048.
- [20] B Lippens. Studies on pore systems in catalysts V. The t method. *Journal of Catalysis*, 4(3):319–323, June 1965. ISSN 00219517. doi: 10.1016/0021-9517(65)90307-6.
- [21] D. Atkinson, A.I. McLeod, and K. S. W. Sing. Adsorptive properties of microporous carbons: Primary and secondary micropore filling. *Journal de Chimie Physique*, 81: 791–794, 1984. ISSN 0021-7689. doi: 10.1051/jcp/1984810791.

- [22] Jean Rouquerol, Gino V. Baron, Renaud Denoyel, Herbert Giesche, Johan Groen, Peter Klobes, Pierre Levitz, Alexander V. Neimark, Sean Rigby, Romas Skudas, Kenneth Sing, Matthias Thommes, and Klaus Unger. The characterization of macroporous solids: An overview of the methodology. *Microporous and Mesoporous Materials*, 154:2–6, May 2012. ISSN 13871811. doi: 10.1016/j.micromeso.2011.09.031.
- [23] D. Dollimore and G.R R. Heal. Pore-size distribution in typical adsorbent systems. *Journal of Colloid and Interface Science*, 33(4):508–519, August 1970. ISSN 00219797. doi: 10.1016/0021-9797(70)90002-0.
- [24] Geza Horvath and Kunitaro Kawazoe. Method for the calculation of effective pore size distribution in molecular sieve carbon. *Journal of Chemical Engineering of Japan*, 16(6):470–475, 1983. ISSN 1881-1299. doi: 10.1252/jcej.16.470.
- [25] A. Saito and H. C. Foley. Curvature and parametric sensitivity in models for adsorption in micropores. *AIChE Journal*, 37(3):429–436, March 1991. ISSN 0001-1541. doi: 10.1002/aic.690370312.
- [26] Andrew D. Wiersum, Estelle Soubeyrand-Lenoir, Qingyuan Yang, Beatrice Moulin, Vincent Guillerm, Mouna Ben Yahia, Sandrine Bourrelly, Alexandre Vimont, Stuart Miller, Christelle Vagner, Marco Daturi, Guillaume Clet, Christian Serre, Guillaume Maurin, and Philip L. Llewellyn. An Evaluation of UiO-66 for Gas-Based Applications. *Chemistry - An Asian Journal*, 6(12):3270–3280, December 2011. ISSN 18614728. doi: 10.1002/asia.201100201.
- [27] Loredana Valenzano, Bartolomeo Civalieri, Sachin Chavan, Silvia Bordiga, Merete H. Nilsen, Søren Jakobsen, Karl Petter Lillerud, and Carlo Lamberti. Disclosing the Complex Structure of UiO-66 Metal Organic Framework: A Synergic Combination of Experiment and Theory. *Chemistry of Materials*, 23(7):1700–1718, April 2011. ISSN 0897-4756. doi: 10.1021/cm1022882.
- [28] Cory M. Simon, Berend Smit, and Maciej Haranczyk. PyIAST: Ideal adsorbed solution theory (IAST) Python package. *Computer Physics Communications*, 200: 364–380, 2016. ISSN 00104655. doi: 10.1016/j.cpc.2015.11.016.
- [29] Jozsef Toth. Uniform Interpretation of Gas/Solid Adsorption. page 239.



# Common characterisation techniques

## 1 Thermogravimetry

Thermogravimetry (TGA) is a standard laboratory technique where the weight of a sample is monitored while ambient temperature is controlled. Changes in sample mass can be correlated to physical events, such as adsorption, desorption, sample decomposition or oxidation, depending on temperature and its rate of change.

TGA experiments are carried out on approximately 15 mg of sample with a TA Instruments Q500 up to 800 °C. The sample is placed on a platinum crucible and sealed in a temperature controlled oven, under gas flow of 40 cm<sup>3</sup> min<sup>-1</sup>. Experiments can use a blanket of either air or argon. The temperature ramp can be specified directly and should be chosen to ensure that the sample is in equilibrium with the oven temperature and no thermal conductivity effects come into play. Alternatively, a dynamic “Hi-Res” mode can be used which allows for automatic cessation of heating rate while the sample undergoes mass loss.

The main purpose of thermogravimetry as used in this thesis is the determination of sample decomposition temperature, to ensure that thermal activation prior to adsorption is complete and that all guest molecules have been removed without loss of structure. To this end, experiments are performed under an inert atmosphere (argon), and the sample activation temperature is chosen as 50 °C to 100 °C lower than the sample decomposition temperature.

## 2 Bulk density determination

Bulk density is a useful metric for the industrial use of adsorbent materials, as their volume plays a critical role in equipment sizing.

Bulk density is determined by weighing 1.5 ml empty glass vessels and settling the MOFs inside. Powder materials are then added in small increments and settled through vibration between each addition. The full vessel is finally weighed, which allowed the bulk density to be determined. The same cell is used in all experiments, with cleaning through sonication between each experiment.

## 3 Skeletal density determination

True density or skeletal density is determined through gas pycnometry in a Microtrac-BEL BELSORP-max apparatus. Helium is chosen as the fluid of choice as it is assumed to be non-adsorbing.

The volume of a glass sample cell ( $V_c$ ) is precisely measured through dosing of the reference volume with helium up to ( $p_1$ ), then opening the valve connecting the two and allowing the gas to expand up to ( $p_2$ ). Afterwards approximately 50 mg of sample are weighed and inserted in a glass sample cell. After sample activation using the supplied electric heater to ensure no solvent residue is left in the pores, the same procedure is repeated to determine the volume of the cell and the adsorbent. With the volume of the sample determined, the density can be calculated by.

$$V_s = V_c + \frac{V_r}{1 - \frac{p_1}{p_2}} \quad (1)$$

## 4 Nitrogen physisorption at 77 K

Nitrogen adsorption experiments are carried out on a Micromeritics Triflex apparatus. Approximately 60 mg of sample are used for each measurement. Empty glass cells are weighed and filled with the samples, which are then activated in a Micromeritics Smart VacPrep up to their respective activation temperature under vacuum and then back-filled with an inert atmosphere. After sample activation, the cells are re-weighed to determine the precise sample mass. The cells are covered with a porous mantle which allows for a constant temperature gradient during measurement by wicking liquid nitrogen around the cell. Finally, the cells are immersed in a liquid nitrogen bath and the adsorption isotherm is recorded using the volumetric method. A separate cell is used to condense the adsorptive throughout the measurement for accurate determination of its saturation pressure.

## 5 Vapour physisorption at 298 K

Vapour adsorption isotherms throughout this work are measured using a MicrotracBEL BELSORP-max apparatus in vapour mode. Glass cells are first weighed and then filled with about 50 mg of sample. The vials are then heated under vacuum up to the activation temperature of the material and re-weighed in order to measure the exact sample mass without adsorbed guests. The cells are then immersed in a mineral oil bath kept at 298 K. To ensure that the cold point of the system occurs in the material and to prevent condensation on cell walls, the reference volume, dead space and vapour source are temperature controlled through an insulated enclosure.

## 6 Gravimetric isotherms

The gravimetric isotherms in this thesis are obtained using a commercial Rubotherm GmbH balance. Approximately 1 g of dried sample is used for these experiments. Samples are activated in situ by heating under vacuum. The gas is introduced using a

step-by-step method, and equilibrium is assumed to have been reached when the variation of weight remained below 30  $\mu\text{g}$  over a 15 min interval. The volume of the sample is determined from a blank experiment with helium as the non-adsorbing gas and used in combination with the gas density measured by the Rubotherm balance to compensate for buoyancy.

# Synthesis method of referenced materials

## 1 Takeda 5A reference carbon

The Takeda 5A carbon was purchased directly from the Takeda corporation. The sample was activated at 250 °C under secondary vacuum (5 mbar) before any measurements.

full  
char-  
acteri-  
zation

## 2 MCM-41 controlled pore glass

MCM-41 (Mobil Composition of Matter No. 41) is a mesoporous silica ( $\text{SiO}_2$ ) material with a narrow pore distribution. First synthesised by the Mobil Oil Corporation, it is produced through templated synthesis using mycelle-forming surfactants. The material referenced in this thesis was purchased from Sigma-Aldrich. The activation procedure consists of heating at 250 °C under secondary vacuum (5 mbar).

## 3 Zr fumarate MOF

The synthesis of the Zr fumarate was performed in Peter Behren's group in Hannover, through modulated synthesis. This MOF can only be synthesised through the addition of a modulator, in this case fumaric acid, to the ongoing reactor, as detailed in the original publication. ( ? )

The procedure goes as follows:  $\text{ZrCl}_4$  (0.517 mmol, 1 eq) and fumaric acid (1.550 mmol, 3 eq) are dissolved in 20 mL N,N-dimethylformamide (DMF) and placed in a 100 mL glass flask at room temperature. 20 equivalents of formic acid were added. The glass flasks were Teflon-capped and heated in an oven at 120 °C for 24 h. After cooling, the white precipitate was washed with 10 mL DMF and 10 mL ethanol, respectively. The washing process was carried out by centrifugation and redispersion of the white powder, which was then dried at room temperature over night

## 4 UiO-66(Zr) for defect study

The UiO-66(Zr) sample preparation was adapted from Shearer et al. ( ? ) as follows:  $\text{ZrCl}_4$  (1.55 g, 6.65 mmol), an excess of terephthalic acid (BDC) (1.68 g, 10.11 mmol), HCl 37 % solution (0.2 mL, 3.25 mmol) and N,N'-dimethylformamide (DMF) (200 mL, 2.58 mol) were added to a 250 mL pressure resistant Schott bottle. The mixture was stirred for 10 min, followed by incubation in a convection oven at 130 °C for 24 h. The resulting white precipitate was washed with fresh DMF (3× 50 mL) followed by ethanol (3× 50 mL) over the course of 48 h and dried at 60 °C. After drying, the sample was

activated on a vacuum oven by heating at 200 °C under vacuum for 12 h. The yield was 78 % white microcrystalline powder. Before the experiment, the sample was calcined at 200 °C under vacuum (5 mbar) to remove any residual solvents from the framework.

## 5 UiO-66(Zr) for shaping study

The scaled-up synthesis of UiO-66(Zr) was carried out in a 5 L glass reactor (Reactor Master, Syrris, equipped with a reflux condenser and a Teflon-lined mechanical stirrer) according to a previously reported method.<sup>(?)</sup> In short, 462 g (2.8 mol) of H<sub>2</sub>BDC (98%) was initially dissolved in 2.5 L of dimethyl formamide (DMF, 2.36 kg, 32.3 mol) at room temperature. Then, 896 g (2.8 mol) of ZrOCl<sub>2</sub> · 8H<sub>2</sub>O (98%) and 465 mL of 37% HCl (548 g, 15 mol) were added to the mixture. The molar ratio of the final ZrOCl<sub>2</sub> · 8H<sub>2</sub>O/H<sub>2</sub>BDC/DMF/HCl mixture was 1 : 1 : 11.6 : 5.4. The reaction mixture was vigorously stirred to obtain a homogeneous gel. The mixture was then heated to 423 K at a rate of 1 K min<sup>-1</sup> and maintained at this temperature for 6 h in the reactor without stirring, leading to a crystalline UiO-66(Zr) solid. The resulting product (510 g) was recovered from the slurry by filtration, redispersed in 7 L of DMF at 333 K for 6 h under stirring, and recovered by filtration. The same procedure was repeated twice, using methanol (MeOH) instead of DMF. The solid product was finally dried at 373 K overnight.

## 6 MIL-100(Fe) for shaping study

The synthesis of the MOF for the shaping study was done at the KRICT institute using a previously published method.<sup>(?)</sup> To synthesise the MIL-100(Fe) material Fe(NO<sub>3</sub>)<sub>3</sub> was completely dissolved in water. Then, trimesic acid (BTC) was added to the solution; the resulting mixture was stirred at room temperature for 1 h. The final composition was Fe(NO<sub>3</sub>)<sub>3</sub> · 9 H<sub>2</sub>O : 0.67 BTC : *n* H<sub>2</sub>O (*x* = 55–280). The reactant mixture was heated at 433 K for 12 h using a Teflon-lined pressure vessel. The synthesized solid was filtered and washed with deionized (DI) water. Further washing was carried out with DI water and ethanol at 343 K for 3 h and purified with a 38 mM NH<sub>4</sub>F solution at 343 K for 3 h. The solid was finally dried overnight at less than 373 K in air.

## 7 MIL-127(Fe) for shaping study

MIL-127(Fe) was synthesized by reaction of Fe(ClO<sub>4</sub>)<sub>3</sub> · 6 H<sub>2</sub>O (3.27 g, 9.2 mmol) and C<sub>16</sub>N<sub>2</sub>O<sub>8</sub>H<sub>6</sub> (3.3 g) in DMF (415 mL) and hydrofluoric acid (5 M, 2.7 mL) at 423 K in a Teflon flask. The obtained orange crystals were placed in DMF (100 mL) and stirred at ambient temperature for 5 h. The final product was kept at 375 K overnight. MIL-127(Fe) was synthesized by reaction of Fe(ClO<sub>4</sub>)<sub>3</sub> · 6 H<sub>2</sub>O (3.27 g, 9.2 mmol) and C<sub>16</sub>N<sub>2</sub>O<sub>8</sub>H<sub>6</sub> (3.3 g) in DMF (415 mL) and hydrofluoric acid (5 M, 2.7 mL) at 423 K in a Teflon flask.

### *Synthesis method of referenced materials*

The obtained orange crystals were placed in DMF (100 mL) and stirred at ambient temperature for 5 h. The final product was kept at 375 K overnight.